Optics Letters

Leaky surface electromagnetic waves on a high-index dielectric grating

A. A. Maradudin,[1] I. Simonsen,[2,*] and W. Zierau[3]

[1]Department of Physics and Astronomy, University of California, Irvine, California 92697, USA
[2]Department of Physics, NTNU Norwegian University of Science and Technology, NO-7941 Trondheim, Norway
[3]Institute for Condensed Matter Theory, University of Muenster, D48149 Muenster, Germany
*Corresponding author: ingve.simonsen@ntnu.no

Received 26 January 2016; revised 29 March 2016; accepted 7 April 2016; posted 7 April 2016 (Doc. ID 256636); published 6 May 2016

We show theoretically that the periodically corrugated surface of a high-index dielectric medium can support a leaky surface electromagnetic wave. This wave is bound to the surface in the vacuum, but radiates into the dielectric. Despite this radiative damping, the surface wave can have a long lifetime.

OCIS codes: (050.0050) Diffraction and gratings; (240.0240) Optics at surfaces; (240.6690) Surface waves.

http://dx.doi.org/10.1364/OL.41.002229

It is well known that a planar vacuum–dielectric interface does not support a surface electromagnetic wave of either p or s polarization when the dielectric constant of the dielectric medium is real and positive. Such a surface also does not support a leaky surface wave. In this Letter, we show that if the vacuum–dielectric interface is periodically corrugated instead of planar and the dielectric constant of the dielectric medium is real, positive, and large, it can support a leaky surface wave. This wave is bound to the surface in the vacuum region but radiates into the dielectric medium.

In order to avoid any misunderstanding, we note that if the dielectric medium has a complex dielectric constant whose real part is positive and constant, and whose imaginary part is positive, constant, and larger than the real part, its planar interface supports a generalized surface wave [1]. However, this wave is attenuated by the ohmic losses in the dielectric. For this reason, we do not consider lossy dielectric media in this Letter.

Our calculations are guided by the following considerations. A periodically corrugated, perfectly conducting surface in contact with vacuum supports a p-polarized surface electromagnetic wave that, in the simplest case, propagates normally to the generators of the surface [2]. If the substrate supporting this wave departs slightly from perfect conductivity, it is tempting to assume that the surface wave is slightly perturbed, but still exists. There are two ways to approach perfect conductivity. The most commonly considered one is to assume a metal at lower and lower frequencies at which the real part of its dielectric function is negative and approaches negative infinity. The second approach is to assume a dielectric medium characterized by a real, positive, frequency-independent dielectric constant that is allowed to become larger and larger.

With the latter approach in mind, in this Letter, we study the propagation of a p-polarized surface electromagnetic wave on a high-index dielectric grating and examine the conditions for its existence. In view of the current interest in alternative plasmonic materials [3], the existence of such a wave on a lossless medium should be of interest.

The physical system we study consists of a dielectric medium whose dielectric constant is ε_1 in the region $x_3 > \zeta(x_1)$ and a dielectric medium whose dielectric constant is ε_2 in the region $x_3 < \zeta(x_1)$. We assume that both ε_1 and ε_2 are real, positive, and frequency independent. The interface profile function $\zeta(x_1)$ is assumed to be single valued, differentiable, and a periodic function of x_1 with period a, $\zeta(x_1 + a) = \zeta(x_1)$. We consider the case of a p-polarized electromagnetic field in this system, whose plane of incidence is the x_1x_3 plane.

We begin by considering the diffraction in reflection and transmission of a plane wave of frequency ω incident from the region $x_3 > \zeta(x_1)$ on the interface $x_3 = \zeta(x_1)$. The dispersion relation for the surface electromagnetic wave supported by the interface can be extracted from the equation for the diffraction amplitudes, while the degree to which the diffracted and refracted fields satisfy unitarity provides an indication of the accuracy of our numerical work.

The single nonzero component of the magnetic field in the region $x_3 > \zeta(x_1)$ that satisfies the boundary conditions as $x_3 \to \infty$ of an incoming incident wave and outgoing diffracted beams, and the Floquet–Bloch condition due to the periodicity of the interface, can be written as

$$H_2^>(x_1, x_3|\omega) = \exp[ikx_1 - i\alpha_1(k,\omega)x_3] + \sum_{n=-\infty}^{\infty} A_n(k,\omega)\exp[ik_n x_1 + i\alpha_1(k_n,\omega)x_3]. \quad (1)$$

Here $k_n = k + 2\pi n/a$ and $\alpha_j(k,\omega) = [\varepsilon_j(\omega/c)^2 - k^2]^{\frac{1}{2}}$. The reduced Rayleigh equation for the diffraction amplitudes $\{A_n(k,\omega)\}$ is [4]

$$\sum_{n=-\infty}^{\infty} M_{mn}(k,\omega)A_n(k,\omega) = -N_m(k,\omega), \qquad m \in \mathbb{N}, \tag{2}$$

where

$$M_{mn}(k,\omega) = \frac{I_{m-n}(\alpha_2(k_m,\omega) - \alpha_1(k_n,\omega))}{\alpha_2(k_m,\omega) - \alpha_1(k_n,\omega)} \times [k_m k_n + \alpha_2(k_m,\omega)\alpha_1(k_n,\omega)], \tag{3a}$$

$$N_m(k,\omega) = \frac{I_m(\alpha_2(k_m,\omega) + \alpha_1(k,\omega))}{\alpha_2(k_m,\omega) + \alpha_1(k,\omega)} \times [k_m k - \alpha_2(k_m,\omega)\alpha_1(k,\omega)]. \tag{3b}$$

In Eq. (3), we have introduced the function

$$I_m(\gamma) = \frac{1}{a}\int_{-\frac{a}{2}}^{\frac{a}{2}} \mathrm{d}x_1 \, \exp\left(-\mathrm{i}\frac{2\pi m}{a}x_1\right)\exp[-\mathrm{i}\gamma\zeta(x_1)]. \tag{4}$$

The manner in which the branch cuts defining the square roots in the definitions of $\alpha_1(k,\omega)$ and $\alpha_2(k,\omega)$ are chosen will be described below.

The diffraction efficiency of the mth scattered beam is defined as the fraction of the total time-averaged incident flux that is diffracted into this beam. It is given by

$$e_m^{(s)} = \frac{\alpha_1(k_m,\omega)}{\alpha_1(k,\omega)}|A_m(k,\omega)|^2. \tag{5}$$

The reflectivity is given by $e_0^{(s)}$.

The single nonzero component of the magnetic field in the region $x_3 < \zeta(x_1)$ that satisfies the boundary condition of outgoing refracted beams as $x_3 \to -\infty$ can be written as

$$H_2^{<}(x_1,x_3|\omega) = \sum_{n=-\infty}^{\infty} B_n(k,\omega)\exp[\mathrm{i}k_n x_1 - \mathrm{i}\alpha_2(k_n,\omega)x_3]. \tag{6}$$

The reduced Rayleigh equation for the refraction amplitudes $\{B_n(k,\omega)\}$ is [4]

$$\sum_{n=-\infty}^{\infty} \frac{I_{m-n}(\alpha_2(k_n,\omega) - \alpha_1(k_m,\omega))}{\alpha_2(k_n,\omega) - \alpha_1(k_m,\omega)} \times [k_m k_n + \alpha_1(k_m,\omega)\alpha_2(k_n,\omega)]B_n(k,\omega) = \delta_{m0}\frac{2\varepsilon_2\alpha_1(k,\omega)}{\varepsilon_2 - \varepsilon_1}, \qquad m \in \mathbb{N}. \tag{7}$$

The refraction efficiency of the mth transmitted beam is

$$e_m^{(t)} = \frac{\varepsilon_1\alpha_2(k_m,\omega)}{\varepsilon_2\alpha_1(k,\omega)}|B_m(k,\omega)|^2. \tag{8}$$

In this lossless structure, the conservation of energy in diffraction and refraction (unitarity) is expressed by

$$\sum_m{}' e_m^{(s)} + \sum_m{}' e_m^{(t)} = 1, \tag{9}$$

where the primes on the sums mean that they are taken over only the open channels, i.e., those for which $\alpha_1(k_m,\omega)$ and $\alpha_2(k_m,\omega)$ are real.

To obtain the dispersion relation for the surface electromagnetic waves by the periodically corrugated interface between two dielectric media, we have only to remove the incident field from the right-hand side of Eq. (1). This is equivalent to deleting the inhomogeneous term from Eq. (2). In this way, we obtain the homogeneous system of equations for the amplitudes $\{A_n(k,\omega)\}$:

$$\sum_{n=-\infty}^{\infty} M_{mn}(k,\omega)A_n(k,\omega) = 0, \qquad m \in \mathbb{N}. \tag{10}$$

The solvability condition for this system of equations, namely the vanishing of the determinant of the matrix $\mathbf{M}(k,\omega)$,

$$D(k,\omega) = \det[M_{mn}(k,\omega)] = 0, \tag{11}$$

is the dispersion relation we seek. The same dispersion relation is obtained from the homogeneous version of Eq. (7).

The magnetic field of the surface wave in medium 1 is then given by the second term on the right-hand side of Eq. (1):

$$H_2^{>}(x_1,x_3|\omega) = \sum_{n=-\infty}^{\infty} A_n(k,\omega)\exp[\mathrm{i}k_n x_1 + \mathrm{i}\alpha_1(k_n,\omega)x_3]. \tag{12}$$

The magnetic field of the surface wave in medium 2 is still given by Eq. (6).

In the determination of the dispersion curve of the surface electromagnetic wave, for specificity, we will assume that the region $x_3 > \zeta(x_1)$ is vacuum, while the region $x_3 < \zeta(x_1)$ is the high-index dielectric medium. Thus we will assume that $\varepsilon_1 = 1$, while $\varepsilon_2 = \varepsilon$. The dispersion curve is insensitive to the interchange $\varepsilon_1 \leftrightarrow \varepsilon_2$.

There are two light lines in this problem. One is the vacuum light line, $\omega = ck$. The wavenumber k has to be larger than ω/c in order that the electromagnetic fields in the vacuum region be bound to the surface. The second light line is the dielectric light line $\omega = ck/\sqrt{\varepsilon}$. The wavenumber k must be larger than $\sqrt{\varepsilon}(\omega/c)$ in order that the electromagnetic field in the dielectric be bound to the surface. In the region between these two light lines, the surface wave is a leaky wave: it is bound to the surface in the vacuum and radiates into the dielectric. The frequency of the wave in this region becomes complex, $\omega = \omega_R - i\omega_I$, with the negative imaginary part reflecting the radiative loss of the energy in the wave as it propagates. Thus we will conduct our search for solutions of Eq. (11) in the region $k > \omega/c$. In this way, we will capture what leaky waves and true surface waves exist.

There is a subtle point here. In order that the surface wave be bound to the surface in the vacuum region and radiate into the dielectric medium, the branch cut defining the square root in the definitions of $\alpha_1(k_n,\omega)$ and $\alpha_2(k_n,\omega)$ must be chosen correctly. Since $\alpha_1^2(k_n,\omega) = [(\omega_R^2 - \omega_I^2)/c^2 - k_n^2] - \mathrm{i}2\omega_R\omega_I/c^2$, we see that it is in the third or fourth quadrant. It has been shown [5] that if the branch cut is taken along the negative imaginary axis, then when $k_n^2 > (\omega_R^2 - \omega_I^2)/c^2$, the nonradiative region, $\alpha_1^2(k_n,\omega)$ is in the third quadrant. This means that $\alpha_1(k_n,\omega)$ will be in the second quadrant with a negative real part and a positive imaginary part. The positive imaginary part of $\alpha_1(k_n,\omega)$ means that the nth term on the right-hand side of Eq. (12) decreases exponentially with increasing x_3, as is required of a surface wave. Similarly, since $\alpha_2^2(k_n,\omega) = [\varepsilon(\omega_R^2 - \omega_I^2)/c^2 - k_n^2] - \mathrm{i}2\varepsilon\omega_R\omega_I/c^2$, we see that it is also in the third or fourth quadrant. If the branch cut is taken along the negative imaginary axis, then when $k_n^2 < \varepsilon(\omega_R^2 - \omega_I^2)/c^2$, the radiative region, $\alpha_2^2(k_n,\omega)$ is in the fourth quadrant. Therefore, $\alpha_2(k_n,\omega)$ is also in the fourth quadrant, with a positive real part and a negative imaginary part. The positive real part of $\alpha_2(k_n,\omega)$ corresponds to a wave that is radiating from the surface into the dielectric medium. The negative imaginary

part of $\alpha_2(k_n, \omega)$ corresponds to a wave whose amplitude increases exponentially with increasing distance into the dielectric from the surface. This exponential increase of the amplitude of a leaky surface wave with increasing distance in the medium into which it is radiating is physically correct. It has been discussed in detail by Lim and Farnell [6], Tonning and Ingebrigtsen [7], and by Glass and Maradudin [8]. The reader is referred to these papers for an explanation of this counterintuitive result.

The solution $\omega(k)$ of the dispersion relation is an even function of k that is periodic in k with a period $2\pi/a$. All of the distinct solutions are obtained if we restrict k to the interval $0 \le k \le \pi/a$. The region of the (ω, k) plane within which surface waves can exist is therefore the triangular region bounded from the left by the vacuum light line $\omega = ck$ and from the right by $k = \pi/a$.

The numerical determination of the dispersion curves for the leaky surface electromagnetic waves supported by the high-index dielectric grating starts by approximating the infinite dimensional equation system Eq. (10) by a finite dimensional system ($|m|, |n| \le \mathcal{N}$). Instead of solving Eq. (11) to obtain the dispersion curves, it is more convenient in numerical calculations to use the fact that $D(k, \omega) = \prod_{n=-\mathcal{N}}^{\mathcal{N}} \lambda_n(k, \omega)$, where $\lambda_n(k, \omega)$ denotes one of the eigenvalues of matrix $\mathbf{M}(k, \omega)$ and solve the equation

$$\Lambda(k, \omega) \equiv \min\{|\lambda_n(k, \omega)|\}_{n=-\mathcal{N}}^{\mathcal{N}} = 0. \tag{13}$$

The region $0 \le k \le \pi/a$ is then divided into $L + 1$ equally spaced points $k_\ell = \ell \Delta k$, with $\ell = 0, 1, 2, \ldots, L$ and $\Delta k = (\pi/a)/L$, and the function $\Lambda(k_\ell, \omega)$ is minimized with respect to the complex angular frequency $\omega(k)$. To this end, we use the Nelder–Mead simplex optimization algorithm [9–11] and treat $\omega_R \ge 0$ and $\omega_I \ge 0$ as two real variables and k_ℓ as a known parameter [5]. For each value of k_ℓ, the minimization starts by assuming $\omega(k_\ell)$ to be on the vacuum light line $k_\ell c$. The values $\omega(k_\ell)$ identified by the algorithm are used to record $\Lambda(k_\ell, \omega(k_\ell))$ and the reciprocal condition number of $\mathbf{M}(k_\ell, \omega(k_\ell))$ to make sure we are on the dispersion curve. In our calculations, these numbers were found to be *at least as small as* 10^{-13} and 10^{-14}, respectively.

In performing the numerical calculations of this work, we assumed the sinusoidal profile function

$$\zeta(x_1) = \zeta_0 \cos\left(\frac{2\pi x_1}{a}\right), \tag{14}$$

where a denotes the period. For this choice, the function $I_m(\gamma)$ defined in Eq. (4) becomes

$$I_m(\gamma) = (-\mathrm{i})^m \mathrm{J}_m(\gamma\zeta_0), \tag{15}$$

where $\mathrm{J}_m(z)$ is the Bessel function of the first kind and order m.

In Fig. 1, we plot the real and imaginary parts of $\omega(k)$ as functions of the wavenumber k for the cases where the surface is a perfect electric conductor (PEC) and where $\varepsilon = 12$, 15, 20, 25, and 50. The value of ζ_0/a assumed in obtaining these six dispersion curves was $\zeta_0/a = 0.10$. A value of $\mathcal{N} = 15$ was used in these calculations. In the upper panel of Fig. 1, the vacuum light line is also indicated. We see from these results that no portion of these dispersion curves lies to the right of the dielectric light lines $\omega = ck/\sqrt{\varepsilon}$ (not indicated in Fig. 1). Consequently, they correspond to leaky surface waves in the entire domain of their existence. We also see that as ε is increased for a fixed value of ζ_0/a, so that the dielectric medium approaches the limit of a PEC, the dispersion curve approaches

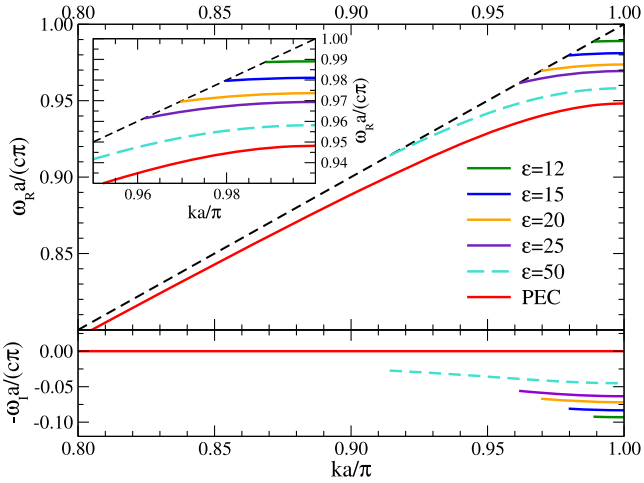

Fig. 1. Real and imaginary parts of $\omega(k)$ are plotted as functions of k for $\varepsilon = 12$, 15, 20, 25 and 50, as well as for a PEC. The vacuum light line is indicated by dashed lines. The inset presents an enlargement of $\omega_R(k)$ in the vicinity of $ka/\pi = 1$ and $\omega a/c\pi = 1$. The parameters assumed in obtaining these results were $\zeta_0/a = 0.10$ and $\mathcal{N} = 15$.

that of the PEC, as it should. This is more clearly seen in the inset of Fig. 1, in which these dispersion curves are enlarged in the vicinity of $ka/\pi = 1$ and $\omega a/c\pi = 1$. It should be stressed that the dispersion curve for the perfect electric conductor shown in Fig. 1 was obtained on the basis of the Rayleigh equation for the system (see Ref. [12], Glass and Maradudin, for details) and not as the $\varepsilon \to \infty$ limit of the reduced Rayleigh equation, Eq. (2). Moreover, it should be remarked that the value $\varepsilon = 50$ assumed for one of the dispersion curves in Fig. 1 probably is unrealistically high. However, it was included in order to more explicitly show the transition toward the PEC limit with increasing ε.

The lower panel of Fig. 1 indicates that the magnitude of $\omega_I(k)$ decreases as the value of ε is increased, as it should, because in the PEC limit, the surface waves it supports have infinite lifetimes. This trend has been confirmed for values of ε larger than those assumed in obtaining Fig. 1. The values of ω_I are of the order $0.05\omega_R$ – $0.10\omega_R$, but can be made smaller by increasing the value of ε.

For several frequencies $\omega = \omega_R(k)$ of the incident light in the range $0.90 < \omega_R(k)a/(c\pi) < 1.00$, we explicitly checked the fulfillment of the energy conservation condition (9). It was found to be satisfied with an error whose magnitude was smaller than 10^{-3}, or better, for all angles of incidence, i.e., in the region to the left of the light line in Fig. 1 and for all values of the dielectric constant assumed in obtaining the results of this figure (including $\varepsilon = 50$). This testifies to the accuracy of the approach used in performing the numerical simulations and therefore in obtaining the dispersion curves depicted in Fig. 1.

We now turn our attention to the excitation/observation of these surface waves. To this end, we study the dependence of the reflectivity and several other low-order diffraction efficiencies on the angle of incidence θ_0. It is well known that in the diffraction of light from a grating that supports a surface wave, these angular dependencies display anomalies of two types. The first, called *Rayleigh anomalies*, occur at values of θ_0 at which a diffraction order appears or disappears in either reflection

($\epsilon = \varepsilon_1$) or transmission ($\epsilon = \varepsilon_2$). These angles are obtained from the relation

$$\sin\theta_0 = \pm\sqrt{\frac{\epsilon}{\varepsilon_1}} - \frac{2m}{\sqrt{\varepsilon_1}}\frac{c\pi}{\omega a}, \tag{16}$$

where ω is the frequency of the incident light and m is an integer. The second type of anomaly, called a *Wood anomaly*, occurs at angles of incidence at which the surface waves are excited through the grating by the incident light. The values of θ_0 at which these anomalies occur are obtained from the relation

$$\sin\theta_0 = \frac{1}{\sqrt{\varepsilon_1}}\frac{c\pi}{\omega a}\left[\pm k_{sw}(\omega)\frac{a}{\pi} - 2m\right]. \tag{17}$$

In this expression, $k_{sw}(\omega)$ is the wavenumber of the surface wave at the frequency ω of the incident light in the region $0 < k_{sw}(\omega) < \pi/a$, and m is an integer. Equations (16) and (17) predict that the angles of incidence at which Rayleigh anomalies in transmission and the angles at which Wood anomalies occur coincide when the frequency ω of the incident light is that of a point on the vacuum light line when $\varepsilon_2 = 1$.

In calculating the angular dependencies of the diffraction efficiencies $e_m^{(s)}$, we have assumed that the medium of incidence is the high-index dielectric material and vacuum is the medium of transmission, as this is a more favorable geometry for the observation of these anomalies. In these calculations, the branch cut defining the square root in $\alpha_j(k, \omega)$ was taken along the negative real axis, and ω and k were real. In solving Eq. (2), we have assumed either (*i*) $\varepsilon_1 = 15$ or (*ii*) $\varepsilon_1 = 20$ and $\varepsilon_2 = 1$. For the wavenumber of the surface waves, we assumed $k_{sw}(\omega)\pi/a = 0.9908$, which corresponds to a frequency of the incident light of (*i*) $\omega a/(c\pi) = 0.9808$ and (*ii*) $\omega a/(c\pi) = 0.9733$, respectively. For these frequencies, leaky surface waves are predicted to exist for $k_{sw}(\omega)$ and complex frequency $\omega_R - i\omega_I$, where $\omega_R = \omega$ and (*i*) $\omega_I a/(c\pi) = 8.2770 \times 10^{-2}$ and (*ii*) $\omega_I a/(c\pi) = 7.1480 \times 10^{-2}$ (see Fig. 1). According to Eq. (17), their existence, for instance, gives rise to Wood anomalies at angles (*i*) $\theta_0 = 15.12°$, 15.41°; and (*ii*) 43.40°, 43.74°. Moreover, Eq. (16) predicts Rayleigh anomalies at (*i*) $\theta_0 = 14.96°$, 15.56°; and (*ii*) $\theta_0 = 43.40°$, 43.74°. Observe that these anomalies are spread over a fairly narrow angular interval of width smaller than 1°; this is a consequence of the dispersion relation for the leaky surface waves being close to the vacuum light line. Additional anomalies are predicted by Eqs. (16) and (17), but they are not discussed here. The values of the remaining parameters assumed in these calculations were $\zeta_0/a = 0.10$ and $\mathcal{N} = 15$. In these calculations, unitarity was checked and was found to be satisfied with an error no larger than 10^{-3}.

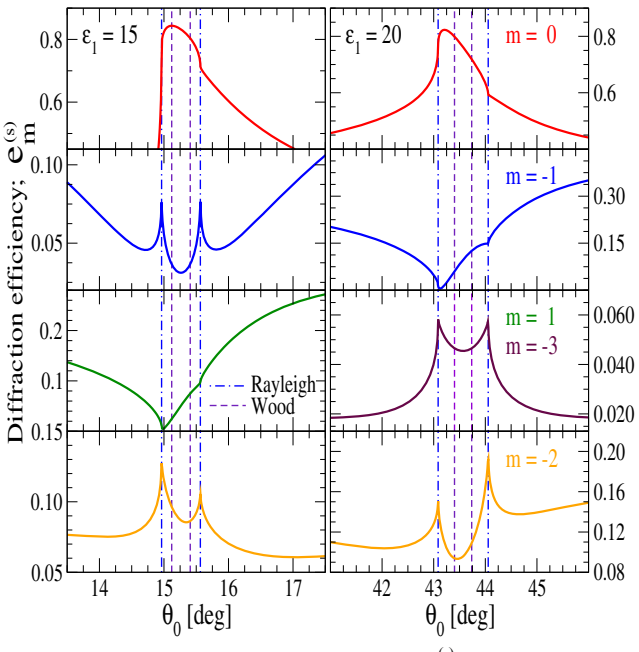

Fig. 2. Diffraction efficiencies in reflection, $e_m^{(s)}$, as functions of the angle of incidence θ_0 for $\varepsilon_1 = 15$ (left column), $\varepsilon_1 = 20$ (right column), and $\varepsilon_2 = 1$. The remaining parameters are given in the text. The angular positions of some of the Rayleigh and Wood anomalies are indicated as dash-dotted and dashed lines, respectively.

In Fig. 2, we have plotted the dependence of $e_m^{(s)}$ on θ_0 for the reflectivity, $m = 0$, for $m = -1$, 1, -2, and -3, and for the two values of ε_1 considered. The agreement between the predicted and observed angles at which Rayleigh anomalies occur is excellent. For the Wood anomalies, the agreement is fair. We believe that this is due to the predicted angular positions of the Wood anomalies being determined from the real part of the surface wave frequency. The imaginary part of the frequency, which is taken into account in the calculation of the diffraction efficiencies, shifts the position of a Wood anomaly and broadens it. The existence of the Wood anomalies demonstrates that it is possible to excite the leaky surface wave with an incident plane wave. Excitation of this wave in the Otto-attenuated, total reflection geometry is also being investigated.

Thus, by a simple calculation, we have shown in this Letter that a periodically corrugated interface between vacuum and a high-index dielectric medium supports a long-lived *p*-polarized leaky surface electromagnetic wave. This result could be applied to gratings fabricated on such high-index dielectric materials as SnO_2 ($\varepsilon = 9.86$ [13]), $Al_{0.6}Ga_{0.4}As$ ($\varepsilon = 10.24$ [14]), silicon ($\varepsilon = 12$), and germanium ($\varepsilon = 16$). These waves could be useful in the fabrication of surface electromagnetic wave-based devices in contexts where a metallic substrate is not suitable, e.g., in an oxidizing atmosphere.

Funding. Research Council of Norway (216699).

REFERENCES

1. F. Yang, J. R. Sambles, and G. W. Bradberry, Phys. Rev. B **44**, 5855 (1991).
2. J. B. Pendry, L. Martn-Moreno, and F. J. Garca-Vidal, Science **305**, 847 (2004).
3. G. Naik, J. Kim, N. Kinsey, and A. Boltasseva, *Modern Plasmonics*, A. A. Maradudin, J. R. Sambles, and W. L. Barnes, eds. (Elsevier, 2014), pp. 189–221.
4. A. A. Maradudin, J. Opt. Soc. Am. **73**, 759 (1983).
5. A. A. Maradudin, I. Simonsen, J. Polanco, and R. M. Fitzgerald, J. Opt. **18**, 024004 (2016).
6. T. C. Lim and G. W. Farnell, J. Acoust. Soc. Am. **45**, 845 (1969).
7. K. A. Ingebrigtsen and A. Tonning, Phys. Rev. **184**, 942 (1969).
8. N. E. Glass and A. A. Maradudin, J. Appl. Phys. **54**, 796 (1983).
9. J. A. Nelder and R. Mead, Comput. J. **7**, 308 (1965).
10. R. O'Neill, Appl. Statist. **20**, 338 (1971).
11. J. C. Lagarias, J. A. Reeds, M. H. Wright, and P. E. Wright, Soc. Ind. Appl. Math. J. Optim. **9**, 112 (1998).
12. N. E. Glass and A. A. Maradudin, Electron. Lett. **17**, 773 (1981).
13. H. J. van Daal, J. Appl. Phys. **39**, 4467 (1968).
14. M. L. Y. Huang, Y. Zhou, and C. J. Chang-Hasnain, Nat. Photonics **1**, 119 (2007).